PAPER • OPEN ACCESS

LiDB: Database of molecular radiative lifetimes for plasma processes

To cite this article: Alec Owens *et al* 2023 *Plasma Sources Sci. Technol.* **32** 085015

View the article online for updates and enhancements.

LiDB: Database of molecular radiative lifetimes for plasma processes

Alec Owens[1,*] , **Tiantian He**[1], **Martin Hanicinec**[1], **Christian Hill**[2] , **Sebastian Mohr**[3] **and Jonathan Tennyson**[1,*]

[1] Department of Physics and Astronomy, University College London, Gower St., London WC1E 6BT, United Kingdom
[2] Atomic and Molecular Data Unit, Division of Physical and Chemical Sciences, International Atomic Energy Agency, Vienna, Austria
[3] Quantemol Ltd, University College London, Gower St., London WC1E 6BT, United Kingdom

E-mail: alec.owens.13@ucl.ac.uk and j.tennyson@ucl.ac.uk

Abstract

LiDB is a newly developed database of molecular vibrational and vibronic state radiative lifetimes. It has been created with the aim of enabling radiative effects to be properly captured in low-temperature plasma models. Datasets have been generated for 36 molecules using comprehensive and highly accurate molecular line lists from the ExoMol spectroscopic database. The main data output of LiDB is radiative lifetimes at vibrational state resolution. Partial lifetimes, which give information on the dominant decay channels in a molecule, are also provided. LiDB is freely available to the scientific community and is hosted at www.exomol.com/lidb. Users can dynamically view molecular datasets or use a specially-designed application programming interface to make data requests. LiDB will continue to expand in the future by adding more molecules, important isotopologues, and neutral and singly-charged atomic species.

Keywords: atomic and molecular data, plasma modelling, database

(Some figures may appear in colour only in the online journal)

1. Introduction

The modelling of radiative decay processes in low-temperature plasmas is a complex and challenging task. Excited atomic and molecular species can exist for vastly differing timescales and emit radiation through a multitude of possible emission pathways, potentially even causing damage in certain plasma applications. For example, in semiconductor fabrication, ultraviolet emissions from the plasma used for etching and deposition can cause radiation damage to the underlying substrate. Properly accounting for radiative effects requires a detailed knowledge of atomic and molecular radiative lifetimes and all possible transition probabilities between the relevant upper and lower states. However, many plasma models ignore the role of radiation, largely because accurate, comprehensive data on radiative lifetimes and emission channels is lacking. Without assessing radiative processes, low-temperature plasmas cannot be reliably optimized for use in a wide range of scientific and industrial applications.

Developing the capabilities to perform full collisional-radiative modelling of technological plasmas would be a significant achievement [1, 2] and is reliant on high-quality input data, the importance of which is being increasingly recognised for simulating low-temperature plasmas [3]. Radiative decay in collisional-radiative modelling has been somewhat

implemented in the CRModel code [4] for atomic or ionic plasma species. The user is able to define transition probabilities, also known as Einstein *A* coefficients, between initial and final states for species of interest. If all decay paths are included then radiative effects are properly accounted for. For atoms, treating radiative decay in this manner is more feasible given the smaller number of electronic transitions that can take place. Literature values, most likely determined by experiment, can be extracted from databases such as the NIST Atomic Spectra Database [5].

Treating molecules is a much more formidable task due to the additional degrees of freedom (rotational, vibrational, electronic). The considerable number of rotation-vibration-electronic (rovibronic) states which may arise leads to a dramatic increase in the number of possible transitions, and hence radiative decay routes. For example, a computed line list for silane (SiH_4) in the wavenumber range 0–5000 cm^{-1} contained just under 62.7 billion transitions between 6.1 million rotation-vibration (rovibrational) energy levels in the electronic ground state [6]. In practice, plasma models are only interested in the dominant radiative decay channels and associated state lifetimes, and are rarely constructed at rotational energy level resolution, thus reducing the data demands substantially.

In this work, we present a new database of molecular vibrational and vibronic state radiative lifetimes, named LiDB. The LiDB database is freely available to the scientific community and can be accessed at www.exomol.com/lidb. Data in LiDB has been generated from existing molecular line lists from the ExoMol database [7–9]. These line lists contain extensive compilations of rovibrational and rovibronic energy levels and all possible transitions between them with associated Einstein *A* coefficients. The line lists are complete up to high temperatures, usually for temperatures much higher than 1000 K, and have been computed using rigorous first-principles computational methods with a degree of empirical tuning to improve the accuracy. This essentially involves rigorously refining the *ab initio* potential energy surface(s) to empirically-derived energy levels, a procedure which can produce orders-of-magnitude improvements in the accuracy of the computed line positions [10, 11]. It is common for there to be hundreds of millions of transitions depending on the size of the molecule. In general, ExoMol line lists are highly accurate, reproducing the fundamental vibrational modes with sub-wavenumber accuracy and line intensities well within 5%–10% of experiment, and often much better [8, 12]. Because of the way in which the ExoMol datasets were computed, it is possible to obtain a complete description of a molecule's radiative properties, and this is one of the key motivations for creating LiDB. Many of the molecular species contained in the ExoMol database are relevant to plasmas. For example, there is a line list available for beryllium monohydride [13] which is important in some fusion plasmas.

The paper is structured as follows: In section 2 we describe the algorithm and methodology used to generate the molecular data in LiDB from the ExoMol line lists. An overview of the LiDB database and how to access molecular datasets is given in section 3. Examples of molecular LiDB radiative lifetimes are presented and discussed in section 4. Finally, in section 5 we conclude and present our future plans for LiDB.

2. Methodology

The radiative lifetime τ_i (in seconds) of a molecular state is defined as,

$$\tau_i = \frac{1}{\sum_f A_{if}}, \tag{1}$$

and is calculated by summing up all the Einstein *A* coefficients A_{if} (in seconds^{-1}) from an initial state i to any connected final state f that is lower in energy. Lifetimes for rovibrational and rovibronic states have previously been computed for a selection of molecules using ExoMol line lists [14]. As mentioned earlier, plasma models are usually constructed at vibrational energy level resolution and do not require rotationally-resolved lifetimes or energies. Thus, for LiDB the goal is to form 'lumped' vibrational or vibronic states, i.e. group together all the rotational energy levels for each vibrational state, and calculate the radiative lifetime for each lumped state. It is also possible to extract information on the allowed decay paths between the lumped states by computing 'partial' lifetimes. These quantities, also in units of seconds, illustrate the dominant emission channels and are provided in LiDB.

The data format of the ExoMol line lists is discussed in detail in the associated publications [8, 9]. Essentially two types of file are used to store line lists. The .states file contains the computed rovibrational and rovibronic energy levels (in cm^{-1}) each labelled with a unique state ID running number and consistent quantum number labelling. The extent of the quantum number labelling will vary depending on the molecule but in most instances each molecular state possesses vibrational state quantum numbers, which facilitates the creation of lumped vibrational states in the LiDB data production algorithm. The .trans file(s) contains the computed transitions from the initial state i (first column in the .trans file) to the final state f (second column), which we will refer to as the upper state u and lower state l, respectively, Einstein *A* coefficients in s^{-1}, and transition wavenumbers ν_{if} in cm^{-1}. The main consideration when computing lifetimes of lumped states is the handling of large datasets of transitions, otherwise it is a relatively straightforward procedure.

2.1. Algorithm to convert ExoMol line lists to LiDB data

We describe the algorithm and background theory used to produce data for LiDB. In summary, for each molecule this involved:

- Creating lumped vibrational states from the rotationally-resolved ExoMol energy levels contained in the .states file.
- Processing the .trans file(s) and determining partial lifetimes for transitions between the lumped vibrational states.

Table 1. List of molecules in LiDB and details of the datasets. N_{elec} is the number of electronic states covered by the dataset, N_{vib} is the number of lumped vibrational states and hence radiative lifetimes, N_{trans} is the number of provided partial lifetimes between the lumped states, E_{thresh} is the upper energy threshold of the LiDB dataset, and the ExoMol line list name and reference is given in the final column. Datasets generated with no energy threshold are marked with a '-' in the E_{thresh} column.

Molecule	Isotopologue	N_{elec}	N_{vib}	N_{trans}	E_{thresh} (eV)	ExoMol line list
AlH	$^{27}Al^1H$	2	30	135	3.719	AlHambra [15]
AlO	$^{27}Al^{16}O$	7	33	150	1.860	ATP [16, 17]
BeH	$^9Be^1H$	2	10	35	1.860	Darby-Lewis [18]
C_2	$^{12}C_2$	8	37	160	1.860	8states [19]
CaH	$^{40}Ca^1H$	3	16	65	1.699	XAB [20]
CaO	$^{40}Ca^{16}O$	5	117	570	2.480	VBATHY [21]
CN	$^{12}C^{14}N$	3	32	145	3.719	Trihybrid [22]
CO	$^{12}C^{16}O$	1	10	35	2.480	Li2015 [23]
CO_2	$^{12}C^{16}O_2$	1	152	733	1.240	UCL-4000 [24]
CS	$^{12}C^{32}S$	1	50	235	—	JnK [25]
H_2	$^1H_2$	1	15	60	—	RACPPK [26]
H_2O	$^1H_2^{16}O$	1	134	655	2.641	POKAZATEL [27]
HCl	$^1H^{35}Cl$	1	18	75	—	HITRAN-HCl [28]
HCN	$^1H^{12}C^{14}N$	1	45	209	0.992	Harris [29]
HF	$^1H^{19}F$	1	10	35	3.719	Coxon-Hajig [30, 31]
KCl	$^{39}K^{35}Cl$	1	121	590	—	Barton [32]
LiH	$^7Li^1H$	1	20	85	2.287	CLT [33]
MgO	$^{24}Mg^{16}O$	5	123	600	2.480	LiTY [34]
NaCl	$^{23}Na^{35}Cl$	1	101	490	—	Barton [32]
NaH	$^{23}Na^1H$	2	10	35	1.100	Rivlin [35]
NaO	$^{23}Na^{16}O$	2	60	285	—	NaOUCMe [36]
NH_3	$^{14}N^1H_3$	1	58	275	0.992	CoYuTe [37]
NO	$^{14}N^{16}O$	3	47	220	6.199	XABC [38]
NS	$^{14}N^{32}S$	1	20	85	2.480	SNaSH [39]
PH	$^{31}P^1H$	2	16	50	2.280	LaTY [40]
PN	$^{31}P^{14}N$	1	27	120	3.719	YYLT [41]
PO	$^{31}P^{16}O$	1	24	105	3.100	POPS [42]
PS	$^{31}P^{32}S$	1	23	100	1.860	POPS [42]
ScH	$^{45}Sc^1H$	6	34	155	1.240	LYT [43]
SH	$^{32}S^1H$	1	16	65	3.447	GYT [44]
SiH	$^{28}Si^1H$	2	10	35	1.860	SiGHTLY [45]
SiH_2	$^{28}Si^1H_2$	1	48	225	0.992	CATS [46]
SiO	$^{28}Si^{16}O$	9	266	1315	7.439	SiOUVenIR [47]
SiS	$^{28}Si^{32}S$	1	35	160	2.853	UCTY [48]
TiO	$^{48}Ti^{16}O$	12	103	465	2.480	Toto [49]
YO	$^{89}Y^{16}O$	6	22	95	1.984	SSYT [50]

- Calculating the total lifetimes of the lumped vibrational states by summing up all the contributions from the partial lifetimes.
- Renormalizing the partial lifetimes to ensure they are consistent with the total lifetimes. This step was necessary as LiDB only provides the five fastest decay paths per lumped vibrational state (discussed below in more detail).

Processing of the ExoMol line lists was performed using a specially designed Python software suite that could be executed directly on the same server hosting the ExoMol database. The procedure was automated and only required molecule-specific input parameters, summarised in table 1, such as the main isotopologue and line list name. Upper radiative state energy thresholds in LiDB were effectively determined by the original line list calculations, namely the 'lower' state energy threshold used when calculating transitions. For example, a lower state threshold of 8000 cm^{-1} in the line list calculations would compute transitions for all states below 8000 cm^{-1} to all the higher energy connected levels. Setting an energy threshold in LiDB ensured that all the radiative decay pathways were accounted for. A number of line lists in the ExoMol database, predominantly diatomic molecules, cover multiple electronic states and for these it was necessary to further group energy levels together within the same electronic state when forming lumped states.

To form the lumped vibrational states, the rotationally-resolved energy levels were grouped together based on their vibrational state quantum numbers and electronic state label. For example, all levels with $v = 1$ in the ground electronic

state were grouped together in a diatomic molecule. Grouping was done on each unique combination of vibrational quanta below the energy threshold. States above the energy threshold were discarded and did not contribute to any further part of the calculation process. An energy was assigned to each grouped set of rotationally-resolved energy levels. This was usually the $J = 0$ energy level value, or the average of the lowest J contributions to that set, e.g. averaging of the energy levels with different parity for $J = 0$. We mention that an energy level lumping procedure was used for carbon dioxide, but instead, lumped *vibrational* states together for modelling plasma-based CO_2 conversion [51].

Only molecules in the ExoMol database with consistent normal mode vibrational quantum numbers were processed. Normal mode quantum numbers are commonly employed in spectroscopic studies but there are some ExoMol line lists, e.g. methane and silane, which use internal vibrational quantum numbers assigned by the computer program (e.g. TROVE [52]) used to generate the line list. There are procedures in place to map the computer-assigned quantum numbers to normal mode notation but it is not always straightforward. However, if users of LiDB identify molecules in the ExoMol database that they require for their applications, please contact us through the LiDB website and we will endeavour to create a consistent set of normal mode vibrational quantum numbers and process the line list for LiDB.

Once the lumped vibrational states were established, it was necessary to calculate the partial lifetimes for the transitions between them. This was achieved by grouping together transitions between the rovibrational energy levels contained in the lumped vibrational states and summing up the individual Einstein A coefficients. The whole procedure was implemented using a Boltzmann averaging scheme to properly account for thermal effects (discussed in more detail below).

To illustrate the procedure it is worthwhile considering a molecule with N lumped vibrational states in total. Each lumped state contains multiple J energy levels (n_u and n_l in total for the upper and lower lumped states, respectively; a different number for each lumped state), corresponding to a set of state ID running numbers in the ExoMol .states file, which we call $\mathbf{u^K} = \{u_1^K, u_2^K, \ldots, u_{n_u}^K\}$ for the upper lumped state U_K for $K = 1, \ldots, N$, and $\mathbf{l^K} = \{l_1^K, l_2^K, \ldots, l_{n_l}^K\}$ for the lower lumped state L_K. In the following we drop the superscript K on the upper and lower rovibrational energy levels.

Focusing on an upper and lower lumped state system, we extracted all the transitions between the upper lumped state set of rovibrational energy levels $\mathbf{u}$ (first column of the ExoMol .trans file) to the lower lumped state set of rovibrational energy levels $\mathbf{l}$ (second column of the .trans file). Any transitions within a lumped state were discarded, e.g. no $u_n \to u_m$ or $l_n \to l_m$ for $n \neq m$. Transitions were grouped on the upper (decaying) state, e.g. $(u_1 \to l_1)$, $(u_1 \to l_2)$, ..., $(u_1 \to l_n)$, and similarly for u_2, ..., u_n, such that the individual contributions to the partial lifetime were computed as,

$$\tau_{u_1, l} = \frac{1}{\sum_{k=1}^n A_{u_1, l_k}}, \tag{2}$$

and

$$\tau_{u_2, l} = \frac{1}{\sum_{k=1}^n A_{u_2, l_k}}, \tag{3}$$

and so on, up to $\tau_{u_n, l}$. Here, A_{u_1, l_1} is the Einstein A coefficient of the transition between the rovibrational levels $u_1 \to l_1$.

To get the partial lifetime $\tau_{U,L}$ between an upper and lower lumped state, it is necessary to form the Boltzmann averaged quantity $< \tau_{u,l} >$ from the multiple individual contributions, defined as

$$\tau_{U,L} = < \tau_{u,l} > = \frac{1}{W} \sum_{k=1}^n \left[\tau_{u_k, l} \times g_{\text{tot}}^{u_k} \exp\left(\frac{-c_2 E_{u_k}}{T}\right) \right], \tag{4}$$

where

$$W = \sum_{k=1}^n g_{\text{tot}}^{u_k} \exp\left(\frac{-c_2 E_{u_k}}{T}\right). \tag{5}$$

Here, E_{u_k} is the energy (in cm^{-1}) of the upper rovibrational state u_k with total statistical degeneracy factor $g_{\text{tot}}^{u_k}$ (which includes any nuclear spin degeneracy resulting from unresolved hyperfine coupling and the $(2J + 1)$ factor from rotational motion). The second radiation constant $c_2 = 1.438775$ cm K and a temperature $T = 700$ K. Note that we assume equilibrium with the translational temperature.

Tests were carried out on aluminium monoxide (AlO), chosen as its lifetimes are known to be more dependent on J [14], and lithium hydride (LiH) to analyse the effect on the final radiative lifetimes from varying the temperature used in the Boltzmann-averaging. Lifetimes were calculated at $T = 300$ K and $T = 1300$ K and compared to the results at $T = 700$ K used in LiDB. For AlO, the lifetimes at $T = 300$ K changed on average by 4.0% compared to the values at $T = 700$ K, and by 9.7% at $T = 1300$ K for the 32 lumped vibrationally excited states. For LiH, the percentages changes were 3.4% (300 K) and 4.4% (1300 K) on average for the 19 lumped vibrationally excited states. The changes in the lifetimes from varying the temperature are small enough that the choice of $T = 700$ K provides a representative thermal distribution for low-temperature plasma applications. As a matter of fact, the Boltzmann averaging procedure does not play a significant role as we are dealing with smaller temperature ranges. If we were averaging over temperatures of several thousands of Kelvin, it would be more meaningful.

Once all the partial lifetimes between the lumped states in a molecule have been established, the total lifetimes of the lumped states can be calculated by summing up all the contributions of the partial lifetimes from an upper lumped state to any connected lower lumped state. At this stage, all the partial lifetimes are considered in the calculation of the total lifetimes. The energy difference between the lower and upper lumped state $\Delta E = E_L - E_U$ was always negative, i.e. corresponding

to radiative decay. Taking an arbitrarily chosen lumped state U_3 as an example, all the partial lifetimes between U_3 and any connected lower lumped states are summed, that is

$$C_3 = \frac{1}{\tau_{U_3,L_0}} + \frac{1}{\tau_{U_3,L_1}} + \frac{1}{\tau_{U_3,L_2}}. \tag{6}$$

The total lifetime τ_{U_3} of the lumped state U_3 is thus,

$$\tau_{U_3} = \frac{1}{C_3}. \tag{7}$$

Generally speaking, this can be expressed as

$$C_K = \sum_{j=0}^{K-1} \frac{1}{\tau_{U_K,L_j}}, \tag{8}$$

and

$$\tau_{U_K} = \frac{1}{C_K}, \tag{9}$$

for $K = 1, \ldots, N$ lumped states.

The number of computed partial lifetimes for a molecule in LiDB can easily number into the thousands and it is very unlikely that any plasma model will be interested in so many decay routes. For this reason, LiDB only provides the five shortest partial lifetimes for each lumped vibrational state. This number was chosen to reduce the size of the datasets while ensuring the main radiative decay routes were captured. Because the total lifetimes are determined from a summation involving all the partial lifetimes, it is necessary to renormalize the five shortest partial lifetimes so that their summation still equals the total lifetime.

Thus, renormalization of the partial lifetimes was performed by computing a renormalization factor R_K (for $K = 1, \ldots, N$ lumped states) based on the ratio between the total lifetime τ_{U_K}, defined in equation (9), and a 'reduced' total lifetime $\tau_{U_K}^*$ obtained from summing up the five shortest partial lifetimes from an upper lumped state, so

$$R_K = \frac{\tau_{U_K}}{\tau_{U_K}^*}. \tag{10}$$

The renormalization factor was then applied to the partial lifetimes, to give renormalized partial lifetimes,

$$\tau_{U_K,L}^* = R_K \times \tau_{U_K,L}, \tag{11}$$

and these are provided in LiDB for the five strongest decays paths from an upper lumped state to the connected lower lumped states. We state that no renormalization is applied to the total lifetimes.

For all molecules in LiDB, the ground vibrational state has an infinite lifetime to radiative decay. Radiative nuclear spin transitions that interconvert ortho and para nuclear spin isomers are currently not considered by the ExoMol database, and therefore not considered in LiDB.

3. Database overview

LiDB is hosted at www.exomol.com/lidb. Users can view molecular datasets dynamically on the website, see Figure 1 and Figure 2, or request data through an API (application programming interface). Basic information on each molecule is provided such as the isotopologue, molecular mass, corresponding ExoMol line list, along with a summary of the dataset such as the number of lumped vibrational states and quantum numbers, whether the data is resolved over multiple electronic states, and so on.

Molecular data is separated into two categories: states and transitions. The states category lists the lumped vibrational states, their state energies (in eV), and the total radiative lifetimes (in seconds). Lumped vibrational states are described by their normal mode vibrational quantum numbers. If the data has been resolved by electronic state, an additional electronic state label is given, otherwise only the ground electronic state has been considered. States are defined using PYVALEM format [53, 54], which is a Python package designed for specifying the species and states of atoms and molecules in a standardized format. For a general discussion of the notation used to designate the different states of molecules the reader is referred to [55, 56]. Users can also view the specific transitions to/from each lumped state.

The transitions category lists at most the five dominant decay channels for each lumped vibrational state, showing the vibrational quanta of the initial and final state, the change in energy ΔE (in eV), which is always negative as the final state is lower in energy than the initial state, and the partial lifetime (in seconds).

Details on how to request data through the API are provided on the website along with examples. Requests are made using the GET protocol and require certain keywords to retrieve the correct molecular data. Requests must be made using the `molecule` keyword to select a specific dataset. Molecular datasets are separated into two categories. Setting the keyword `category = states` will request total radiative lifetimes (in seconds) for the lumped vibrational states, while `category = transitions` will request partial lifetimes (in seconds) between the lumped vibrational states. Data can be returned in either JSON (default) or CSV format. For example, radiative lifetimes of the CaO molecule in CSV format can be requested as: www.exomol.com/lidb/api/?molecule=CaO&category=states&format=csv and this will return a comma-separated values file with three columns listing the molecular state (PyValem notation), lifetime (in seconds) and energy (in eV).

4. Results and discussion

As mentioned earlier, radiative lifetimes of rovibrational and rovibronic states have been computed for some of the molecules in the ExoMol database [14]. To assess the LiDB vibrational state lumping procedure and calculation of total

Figure 1. Screenshot of the LiDB website at www.exomol.com/lidb. Users can view molecular datasets dynamically or use the API to query the database.

radiative lifetimes, it is informative to compare against the rotationally-resolved results.

In figure 3, total radiative lifetimes τ are plotted for three electronic states of NO, comparing LiDB values against the rovibronic values of the ExoMol NO line list XABC [38]. LiDB values closely follow the XABC lifetimes and gradually decrease in value with increasing energy, behaviour which is somewhat expected as higher vibrational states will usually decay faster. The LiDB lifetime for each lumped vibrational state tends to have a value close to the lower-J lifetimes of the XABC results. This is because we have used a temperature of $T = 700$ K, corresponding to a maximum in the Boltzmann averaging, see equation (4), of NO at $J \approx 16.5$, which is much lower than the maximum value in the XABC line list of $J = 184.5$. Lifetimes of the electronically excited states are several orders of magnitude smaller than the ground state, demonstrating that these states are comparatively short-lived. It should be noted that in

all figures the infinite lifetime of the ground state is not shown.

In figure 4, total radiative lifetimes are shown for five electronic states of CaO, comparing LiDB values against the rovibronic values of the ExoMol CaO VBATHY line list [21]. The original CaO lifetimes are considerably more spread out, showing much greater variation compared to NO in figure 3. Notably, in the lower panels of figure 4 showing the $a^3\Pi$ and $b^3\Sigma^+$ electronic states, some of the LiDB lifetimes appear larger in magnitude than the original ExoMol values from which they were formed (through the lumping procedure). This behaviour is unphysical and unfortunately an artefact of the underlying vibrational state quantum number labelling in the VBATHY line list. The excited electronic states in CaO cross and interact with each other at certain bond lengths, see figure 1 of [21]. These interactions cause mixing between the different vibrational states, making them harder to reliably assign in the underlying variational nuclear

States of CaO				
		Search:		
Electronic state	Vibrational state: v	Energy (eV)	Lifetime (s)	Transition
$b^3\Sigma^+$	0	1.181	7.21e-03	5
$X^1\Sigma^+$	0	0.000	∞	
$A'^1\Pi$	0	1.067	6.98e-05	5
$A^1\Sigma^+$	0	1.432	1.07e-07	5
$a^3\Pi$	0	1.035	7.80e-02	5
$X^1\Sigma^+$	1	0.090	1.28e-01	1
$b^3\Sigma^+$	1	1.251	4.75e-03	5
$A'^1\Pi$	1	1.134	4.70e-05	5
$a^3\Pi$	1	1.102	4.46e-02	5
$A^1\Sigma^+$	1	1.520	1.22e-07	5
$A^1\Sigma^+$	2	1.608	1.29e-07	5
$b^3\Sigma^+$	2	1.321	7.18e-03	5
$A'^1\Pi$	2	1.202	4.01e-05	5
$a^3\Pi$	2	1.168	2.97e-02	5
$X^1\Sigma^+$	2	0.178	4.50e-02	2
Electronic state	Vibrational state	Energy (eV)	Lifetime (s)	Transition

Showing 1 to 15 of 117 entries

Transitions of NH_3			
		Search:	
Initial state	Final state	ΔE (eV)	Partial lifetime (s)
$v=(0, 0, 0, 1)$	$v=(0, 0, 0, 0)$	-0.202	2.18e-01
$v=(0, 0, 0, 1)$	$v=(0, 1, 0, 0)$	-0.084	1.05e+01
$v=(0, 0, 0, 2)$	$v=(0, 0, 0, 0)$	-0.400	1.62e+00
$v=(0, 0, 0, 2)$	$v=(0, 0, 0, 1)$	-0.199	2.00e-01
$v=(0, 0, 0, 2)$	$v=(0, 1, 0, 0)$	-0.282	2.39e+01
$v=(0, 0, 0, 2)$	$v=(0, 1, 0, 1)$	-0.083	3.31e+00
$v=(0, 0, 0, 2)$	$v=(0, 2, 0, 0)$	-0.185	1.31e+02
$v=(0, 0, 0, 3)$	$v=(0, 0, 0, 1)$	-0.397	9.87e-01
$v=(0, 0, 0, 3)$	$v=(0, 0, 0, 2)$	-0.198	1.10e-01
$v=(0, 0, 0, 3)$	$v=(0, 1, 0, 1)$	-0.281	8.13e+00
$v=(0, 0, 0, 3)$	$v=(0, 1, 0, 2)$	-0.084	1.66e+00
$v=(0, 0, 0, 3)$	$v=(0, 2, 0, 1)$	-0.184	3.99e+01
$v=(0, 0, 0, 4)$	$v=(0, 0, 0, 2)$	-0.392	5.75e-01
$v=(0, 0, 0, 4)$	$v=(0, 0, 0, 3)$	-0.194	1.01e-01
$v=(0, 0, 0, 4)$	$v=(0, 1, 0, 2)$	-0.278	4.39e+00
Initial state	Final state	ΔE (eV)	Partial lifetime (s)

Showing 1 to 15 of 275 entries

Figure 2. Screenshot of the LiDB website at www.exomol.com/lidb. The left panel shows lumped states and total radiative lifetimes of CaO. The right panel shows transitions between the lumped states and partial lifetimes of NH_3.
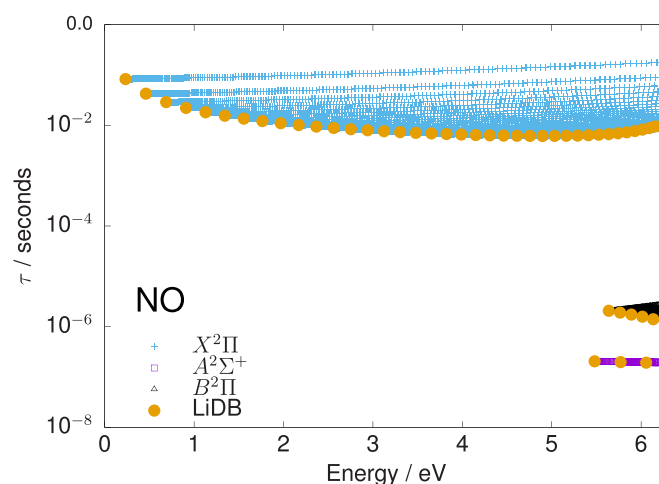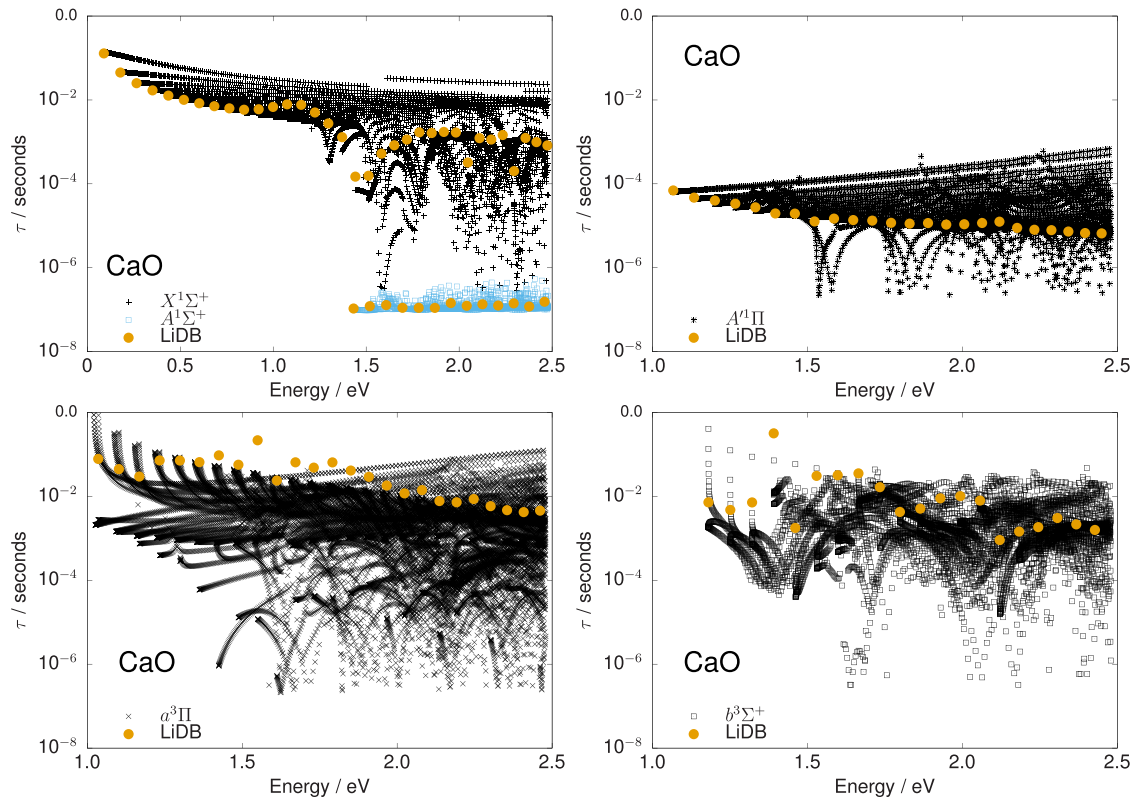

Figure 3. Comparison of nitric oxide (NO) radiative lifetimes τ (in seconds) for rotationally-resolved values from the ExoMol NO line list XABC [38] and lumped vibrational state values from LiDB. Lifetimes in three electronic states of NO are shown. Note that the lifetime of the ground vibrational state is infinite and has not been plotted.

motion calculations used to generate the line list. Generally speaking, assignment in variational nuclear motion calculations is done by analysing the contribution of the underlying basis functions used to determine the energy level, and in instances where there are strong interactions between the electronic states or high levels of vibrational excitation, this assignment can be ambiguous. As an example, in CaO the LiDB lifetimes are above the ExoMol values for the $v = 7$ $(a^3\Pi)$ and $v = 4$ $(b^3\Sigma^+)$ states, which in the original VBATHY line list have $J = 0$ energy levels around $\approx 12\,000\,\text{cm}^{-1}$. Given the lumping procedure considers all rotationally-excited levels, it is very likely that there has been misassignments and this is causing the over-estimated lifetimes in LiDB. These instances are rare in LiDB and should only be small in magnitude.

In figure 5, LiDB lifetimes are illustrated for SiH_2, H_2O, CO_2 and NH_3. The SiH_2 and NH_3 lifetimes show relatively straightforward behaviour and decrease in value with increasing energy. For H_2O, the lifetimes actually increase with energy but caution must be exercised when using these data, as the behaviour is an artefact of the underlying ExoMol POKAZATEL water line list [27]. The POKAZATEL line list does not have full vibrational state quantum number labelling and many of the highly excited rovibrational states are unassigned. The LiDB data generation algorithm would have discarded the unassigned states, hence certain radiative decay channels will be missing and the lifetimes will be longer-lived. Given the importance of water, we have included this molecule in LiDB but we recommend caution if using H_2O

Figure 4. Comparison of calcium oxide (CaO) radiative lifetimes τ (in seconds) for rotationally-resolved values from the ExoMol CaO line list VBATHY [21] and lumped vibrational state values from LiDB. Lifetimes in five electronic states of CaO are shown. Note that the lifetime of the ground vibrational state is infinite and has not been plotted.
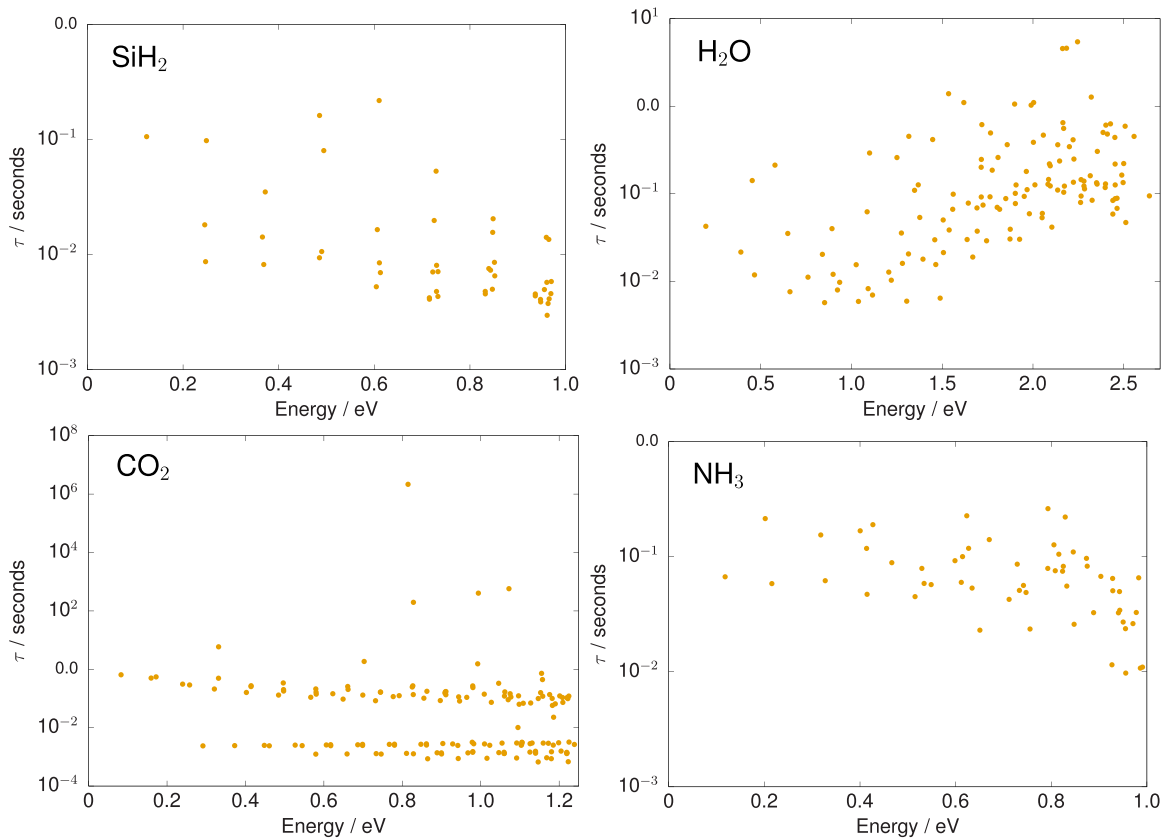
Figure 5. Radiative lifetimes τ (in seconds) from LiDB for lumped vibrational states of silylene (SiH$_2$), water (H$_2$O), carbon dioxide (CO$_2$) and ammonia (NH$_3$). Note that the lifetime of the ground vibrational state is infinite and has not been plotted.i.

data above energies with 1.5 eV. No other molecule in LiDB suffers from the issue of partial quantum number labelling. Finally, interesting behaviour is seen for CO_2 which possesses a number of considerably long-lived states. Notably, the excited bending mode of CO_2 with vibrational quanta $v_2 = 10$ at 0.815 eV has a radiative lifetime of $\tau = 2.2 \times 10^6$ s.

5. Conclusions and outlook

A new database of molecular radiative lifetimes has been presented. Data in LiDB has been generated from highly accurate and comprehensive molecular line lists from the ExoMol database. An efficient algorithm was designed to form lumped vibrational states from rotationally-resolved energy levels. The total radiative lifetimes of the lumped states were established and these values are the major data output of LiDB. Partial lifetimes, which give information on the dominant decay channels from a lumped state, are also provided by LiDB. Given the huge possible number of decay paths, only five partial lifetimes per lumped state are provided which have been renormalized so as to add up to the total lifetime. LiDB is freely available to the scientific community and can be accessed at www.exomol.com/lidb. An API has been designed to enable user-requests of data, or data can be dynamically viewed on the website.

Currently LiDB contains 36 molecules and we plan to add new species in the future including important isotopologues. The choice of 36 molecules was effectively decided by those available in the ExoMol database with meaningful vibrational state quantum number labelling. As discussed earlier, it is essential to have a consistent set of meaningful vibrational state quantum numbers for all the energy levels and this is not the case for certain polyatomic molecules. Work is underway to rectify this for key plasma species such as silane. We encourage the community to contact us with recommendations of data that they would like in LiDB, or suggestions for ways to improve the functionality and accessibility of the database and website.

Some of the datasets in LiDB are based on line lists without complete coverage, for example, for CO we could only reliably provide lifetimes for the lowest nine lumped vibrational levels using the line list of [23]. A more comprehensive CO line list is currently being worked on as part of the ExoMol project and LiDB will be updated when this becomes available. Similarly, LiDB lifetimes for H_2 were based on the ground electronic state line list of [26] but we are planning to include vibronic transitions in the future and the respective lifetimes will be added accordingly.

Atoms are an essential component of any plasma model and we are in the process of incorporating atomic radiative lifetime data into LiDB. LiDB will initially offer neutral and singly-charged species with the atomic data generated from energy levels and transition probabilities from the NIST Atomic Spectra Database [5].

One important future development will be the inclusion of radiative LiDB data into the Quantemol database (QDB) of plasma chemistries and reactions [57], which some of the authors are involved with. QDB provides cross sections and rates of processes important for plasma models involving heavy particle collisions (chemical reactions) and electron collision processes. Work on this is in progress.

Data availability statement

The data that support the findings of this study are openly available at the following URL/DOI: www.exomol.com/lidb/molecule/list/all/.

ORCID iDs

Alec Owens https://orcid.org/0000-0002-5167-983X
Christian Hill https://orcid.org/0000-0001-6604-0126
Jonathan Tennyson https://orcid.org/0000-0002-4994-5238

References

[1] Adamovich I *et al* 2022 *J. Appl. Phys.* **55** 373001
[2] Lu X *et al* 2022 *Front. Phys.* **10** 1040658
[3] Alves L L *et al* 2023 *Plasma Sources Sci. Technol.* **32** 023001
[4] Hartgers A, van Dijk J, Jonkers J and van der Mullen J 2001 *Comput. Phys. Commun.* **135** 199–218
[5] Kramida A, Yu R and Reader J (NIST ASD Team) 2022 NIST atomic spectra database (ver. 5.10) (available at: https://physics.nist.gov/asd) (Accessed 31 January 2016) National Institute of Standards and Technology, Gaithersburg, MD
[6] Owens A, Yurchenko S N, Yachmenev A, Thiel W and Tennyson J 2017 *Mon. Not. R. Astron. Soc.* **471** 5025–32
[7] Tennyson J and Yurchenko S N 2012 *Mon. Not. R. Astron. Soc.* **425** 21–33
[8] Tennyson J *et al* 2016 *J. Mol. Spectrosc.* **327** 73–94
[9] Tennyson J *et al* 2020 *J. Quant. Spectrosc. Radiat. Transf.* **255** 107228
[10] Yurchenko S N, Barber R J, Tennyson J, Thiel W and Jensen P 2011 *J. Mol. Spectrosc.* **268** 123–9
[11] Tennyson J 2012 *WIREs Comput. Mol. Sci.* **2** 698–715
[12] Bielska K *et al* 2022 *Phys. Rev. Lett.* **129** 043002
[13] Darby-Lewis D, Tennyson J, Yurchenko S N and Lawson K D 2020 *J. Phys. B: At. Mol. Opt. Phys.* **53** 135202
[14] Tennyson J, Hulme K, Naim O K and Yurchenko S N 2016 *J. Phys. B: At. Mol. Opt. Phys.* **49** 044002
[15] Yurchenko S N, Williams H, Leyland P C, Lodi L and Tennyson J 2018 *Mon. Not. R. Astron. Soc.* **479** 1401–11
[16] Patrascu A T, Tennyson J and Yurchenko S N 2015 *Mon. Not. R. Astron. Soc.* **449** 3613–9
[17] Bowesman C A, Shuai M, Yurchenko S N and Tennyson J 2021 *Mon. Not. R. Astron. Soc.* **508** 3181–93
[18] Darby-Lewis D, Tennyson J, Lawson K D, Yurchenko S N, Stamp M F, Shaw A and Brezinsek S (JET Contributor) 2018 *J. Phys. B: At. Mol. Opt. Phys.* **51** 185701

[19] Yurchenko S N, Szabo I, Pyatenko E and Tennyson J 2018 *Mon. Not. R. Astron. Soc.* **480** 3397–411

[20] Owens A, Dooley S, McLaughlin L, Tan B, Zhang G, Yurchenko S N and Tennyson J 2022 *Mon. Not. R. Astron. Soc.* **511** 5448–61

[21] Yurchenko S N, Blissett A, Asari U, Vasilios M, Hill C and Tennyson J 2016 *Mon. Not. R. Astron. Soc.* **456** 4524–32

[22] Syme A M and McKemmish L K 2021 *Mon. Not. R. Astron. Soc.* **505** 4383–95

[23] Li G, Gordon I E, Rothman L S, Tan Y, Hu S M, Kassi S, Campargue A and Medvedev E S 2015 *Astrophys. J. Suppl.* **216** 15

[24] Yurchenko S N, Mellor T M, Freedman R S and Tennyson J 2020 *Mon. Not. R. Astron. Soc.* **496** 5282–91

[25] Paulose G, Barton E J, Yurchenko S N and Tennyson J 2015 *Mon. Not. R. Astron. Soc.* **454** 1931–9

[26] Roueff E, Abgrall H, Czachorowski P, Pachucki K, Puchalski M and Komasa J 2019 *Astron. Astrophys.* **630** A58

[27] Polyansky O L, Kyuberis A A, Zobov N F, Tennyson J, Yurchenko S N and Lodi L 2018 *Mon. Not. R. Astron. Soc.* **480** 2597–608

[28] Gordon I E *et al* 2017 *J. Quant. Spectrosc. Radiat. Transf.* **203** 3–69

[29] Barber R J, Strange J K, Hill C, Polyansky O L, Mellau G C, Yurchenko S N and Tennyson J 2014 *Mon. Not. R. Astron. Soc.* **437** 1828–35

[30] Li G, Gordon I E, Le Roy R J, Hajigeorgiou P G, Coxon J A, Bernath P F and Rothman L S 2013 *J. Quant. Spectrosc. Radiat. Transf.* **121** 78–90

[31] Coxon J A and Hajigeorgiou P G 2015 *J. Quant. Spectrosc. Radiat. Transf.* **151** 133–54

[32] Barton E J, Chiu C, Golpayegani S, Yurchenko S N, Tennyson J, Frohman D J and Bernath P F 2014 *Mon. Not. R. Astron. Soc.* **442** 1821–9

[33] Coppola C M, Lodi L and Tennyson J 2011 *Mon. Not. R. Astron. Soc.* **415** 487–93

[34] Li H Y, Tennyson J and Yurchenko S N 2019 *Mon. Not. R. Astron. Soc.* **486** 2351–65

[35] Rivlin T, Lodi L, Yurchenko S N, Tennyson J and Le Roy R J 2015 *Mon. Not. R. Astron. Soc.* **451** 5153–7

[36] Mitev G B, Taylor S, Tennyson J, Yurchenko S N, Buchachenko A A and Stolyarov A V 2022 *Mon. Not. R. Astron. Soc.* **511** 2349–55

[37] Coles P A, Yurchenko S N and Tennyson J 2019 *Mon. Not. R. Astron. Soc.* **490** 4638–47

[38] Qu Q, Yurchenko S N and Tennyson J 2021 *Mon. Not. R. Astron. Soc.* **504** 5768–77

[39] Yurchenko S N, Bond W, Gorman M N, Lodi L, McKemmish L K, Nunn W, Shah R and Tennyson J 2018 *Mon. Not. R. Astron. Soc.* **478** 270–82

[40] Langleben J, Yurchenko S N and Tennyson J 2019 *Mon. Not. R. Astron. Soc.* **488** 2332

[41] Yorke L, Yurchenko S N, Lodi L and Tennyson J 2014 *Mon. Not. R. Astron. Soc.* **445** 1383–91

[42] Prajapat L, Jagoda P, Lodi L, Gorman M N, Yurchenko S N and Tennyson J 2017 *Mon. Not. R. Astron. Soc.* **472** 3648–58

[43] Lodi L, Yurchenko S N and Tennyson J 2015 *Mol. Phys.* **113** 1559–75

[44] Gorman M, Yurchenko S N and Tennyson J 2019 *Mon. Not. R. Astron. Soc.* **490** 1652–65

[45] Yurchenko S N, Sinden F, Lodi L, Hill C, Gorman M N and Tennyson J 2018 *Mon. Not. R. Astron. Soc.* **473** 5324–33

[46] Clark V H J, Owens A, Tennyson J and Yurchenko S N 2020 *J. Quant. Spectrosc. Radiat. Transf.* **246** 106929

[47] Yurchenko S N *et al* 2022 *Mon. Not. R. Astron. Soc.* **510** 903–19

[48] Upadhyay A, Conway E K, Tennyson J and Yurchenko S N 2018 *Mon. Not. R. Astron. Soc.* **477** 1520–7

[49] McKemmish L K, Masseron T, Hoeijmakers J, Pérez-Mesa V V, Grimm S L, Yurchenko S N and Tennyson J 2019 *Mon. Not. R. Astron. Soc.* **488** 2836–54

[50] Yurchenko S N, Smirnov A N, Solomonik V G and Tennyson J 2019 *Phys. Chem. Chem. Phys.* **21** 22794–810

[51] Berthelot A and Bogaerts A 2016 *Plasma Sources Sci. Technol.* **25** 045022

[52] Yurchenko S N, Thiel W and Jensen P 2007 *J. Mol. Spectrosc.* **245** 126–40

[53] Hill C 2019 Technical meeting on the development of software programs and database tools for modelling edge plasma processes in fusion devices; appendix 5: Draft standards for the representation of atomic and molecular species and states in databases *Technical Report* (IAEA) (available at: www-nds.iaea.org/publications/indc/indc-nds-0805.pdf)

[54] Hill C 2019 PyValem: a Python package for parsing, validating, manipulating and interpreting the chemical formulas, quantum states and labels of atoms, ions and small molecules (available at: https://github.com/xnx/pyvalem)

[55] Bernath P F 2015 *Spectra of Atoms and Molecules* 3rd edn (Oxford University Press)

[56] Tennyson J 2019 *Astronomical Spectroscopy : An Introduction to the Atomic and Molecular Physics of Astronomical Spectra* 3rd edn (World Scientific)

[57] Tennyson J *et al* 2022 *Plasma Sources Sci. Technol.* **31** 095020